



LAWRENCE
LIVERMORE
NATIONAL
LABORATORY

Deflagration Behavior of HMX-Based Explosives at High Temperatures and Pressures

Jon L. Maienschein, Jeffrey F. Wardell

November 21, 2003

JANNAF 21st Propulsion Systems Hazards Subcommittee
Meeting
Colorado Springs, CO, United States
December 2, 2003 through December 4, 2003

Disclaimer

This document was prepared as an account of work sponsored by an agency of the United States Government. Neither the United States Government nor the University of California nor any of their employees, makes any warranty, express or implied, or assumes any legal liability or responsibility for the accuracy, completeness, or usefulness of any information, apparatus, product, or process disclosed, or represents that its use would not infringe privately owned rights. Reference herein to any specific commercial product, process, or service by trade name, trademark, manufacturer, or otherwise, does not necessarily constitute or imply its endorsement, recommendation, or favoring by the United States Government or the University of California. The views and opinions of authors expressed herein do not necessarily state or reflect those of the United States Government or the University of California, and shall not be used for advertising or product endorsement purposes.

DEFLAGRATION BEHAVIOR OF HMX-BASED EXPLOSIVES AT HIGH TEMPERATURES AND PRESSURES[□]

J.L. Maienschein and J.F. Wardell

Lawrence Livermore National Laboratory

Livermore, CA[□]

ABSTRACT

We report the deflagration behavior of several HMX-based explosives at pressure from 10-600 MPa and temperatures from 20-180°C. We have made laminar burn rate measurements with the LLNL High Pressure Strand Burner, in which burn wires are used to record the time-of-arrival of the burn front in the cylindrical sample as a function of pressure. The explosive samples are 6.4 mm in diameter and 63 mm long, with ten burn wires embedded at different positions in the sample. Burning on the cylindrical surface is inhibited with an epoxy layer. With this direct measurement we do not have to account for product gas equation of state or heat losses in the system, and the burn wires allow detection of irregular burning. We find that formulation details are very important to overall deflagration behavior - the presence of 10% or less by weight of binder leads to physical deconsolidation and rapid deflagration at high pressures, and a larger particle size distribution leads to slower deflagration. High temperatures have a relatively minor effect on the deflagration rate until the beta-to-delta phase transition temperature is reached, beyond which the deflagration rate increases approximately 40-fold.

INTRODUCTION

An explosive when heated to a sufficiently high temperature, either intentionally or unintentionally (such as in a fire), will produce a thermal explosion or in some cases a detonation, resulting in a great deal of damage. A thermal explosion is a violent event caused by thermal ignition of the explosive charge and is characterized by the sub-sonic propagation of a deflagration reaction through the explosive. (In some very unusual circumstances, a thermally-drive reaction may lead to a detonation, characterized by supersonic propagation of the reaction.) During a thermal explosion, the deflagration propagates at high pressures (up to several kbar) and temperatures (1000 K or more), and in the case of slow cookoff through explosive that has been degraded by prolonged exposure to high temperature.

The violence of the thermal explosion depends greatly on the behavior of the explosive. Materials that exhibit rapid deflagration (particularly in a damaged state) tend to give more violent thermal explosions. Experimental characterization of deflagration behavior at high pressure and temperature, for pristine and degraded materials, provides critical information on the propagation of thermal explosions.

□

Distribution Statement A: Approved for public release; distribution is unlimited.

This work was performed under the auspices of the U.S. Department of Energy by Lawrence Livermore National Laboratory under contract No. W-7405-ENG-48.

Here we report experimental characterization of the deflagration behavior of several HMX-based explosives at pressures from 10-600 MPa and temperatures from 20-180°C, including samples that were subject to severe thermal degradation. We also draw conclusions concerning the effect of several material variables on deflagration behavior, which may allow extrapolation of results to families of similar materials.

EXPERIMENTS

LLNL HIGH PRESSURE STRAND BURNER

The LLNL high pressure strand burner, shown schematically in Figure 1, combines the features of a traditional closed-bomb burner with those of a traditional strand burner. The LLNL high-pressure strand burner contains a burning sample in a small volume, high-pressure chamber. We measure temporal pressure data and burn front time-of-arrival data to get the laminar burn rate for a range of pressures in one experiment. We use a pressure transducer and a load cell to measure the temporal pressure in the bomb, and detect the arrival of the burn front by the burning-through of thin wires embedded in the sample. High speed digital scopes captures the data for subsequent analysis. The combination of pressure and flame front location data allows us to determine if a sample burns in a uniform laminar fashion or if the burn front propagates through in a more erratic nature, for example caused by physical disruption of the sample. This provides a complete picture of the deflagration process, which is otherwise difficult to obtain at these high pressures. In contrast, with a standard closed-bomb burner pressure in the combustion chamber is the only measurement; calculation of the burn rate requires accurate knowledge of the equation of state of the product gases and accurate treatment of heat losses. There is no measure of the surface regression rate to check combustion uniformity, so data from samples that burn erratically are particularly hard to interpret. The standard strand burner provides direct measurement of the surface regression rate in a large volume at constant pressure, giving only one pressure/rate data point in each experiment; furthermore, the large volume required for isobaric operation means that operation at high pressures is generally not practical.

The strand burner has a volume of about 75 cm³, and is designed to reach pressures of 1 GPa (150,000 psi). The pressure vessel body is built from two concentric shells with interference between them to put the inner shell in compression. The shells and the top and bottom closures are fabricated from hardened S-5 tool steel, which is suitable for HMX-based explosives which generate little or no corrosive gases. The burn sample, shown in Figure 2, is a cylinder ~60 mm long and 6.4 mm in diameter, made of nine cylindrical propellant pellets stacked on end; silver burn wires (75 μm diameter) are inserted between each pair of pellets, in a groove in each pellet. After assembly, the cylindrical surface of the sample is coated with epoxy (Epon 828 with Versamid 140 catalyst) to prevent burning of this surface; this limits the burn front to the end of the cylinder, resulting in a laminar burn. The sample end is ignited by a thin HNS pressed pellet (30 mg), which is in turn ignited by a hot wire and 130 mg of boron potassium nitrate.

To conduct a measurement, the burn sample is inserted into the pressure vessel. The sample mounts into a pre-wired base that carries the signal wires through high-pressure feedthroughs in the bottom plug of the pressure vessel. The system is pressurized to the desired starting pressure (up to 400 MPa or 60,000 psi) with argon, and then burned while recording data. Typical pressure and flame front time-of-arrival data are shown in Figure 3. One noteworthy feature is the use of solid argon plugs as the remotely-actuated pressure isolation valves. Once the system is pressurized (using manual valves), it is isolated with solid argon plugs by immersing sections of the inlet and outlet tubing in liquid nitrogen. The manual valves are then opened prior to going to remote operation for the burn. Following the burn, the pressure is released by remotely removing the liquid nitrogen from the outlet tubing. The solid argon plugs provide a reliable remotely-actuated valve for high-pressure gas with no moving parts and no seals to maintain. Additional details on the apparatus have been previously published.¹⁻³

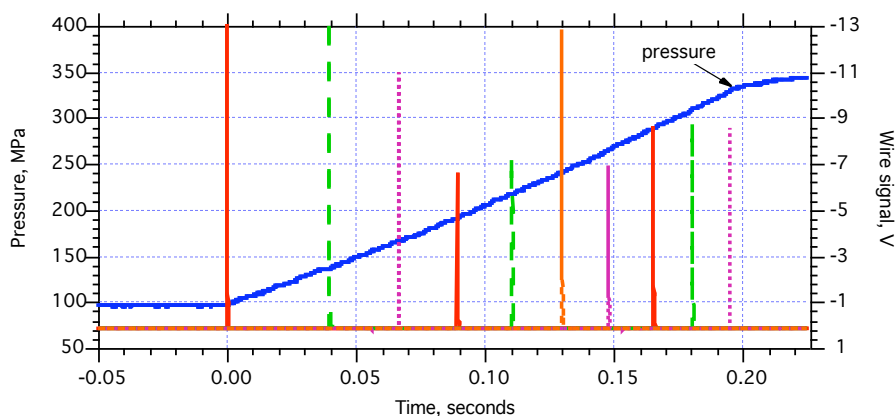
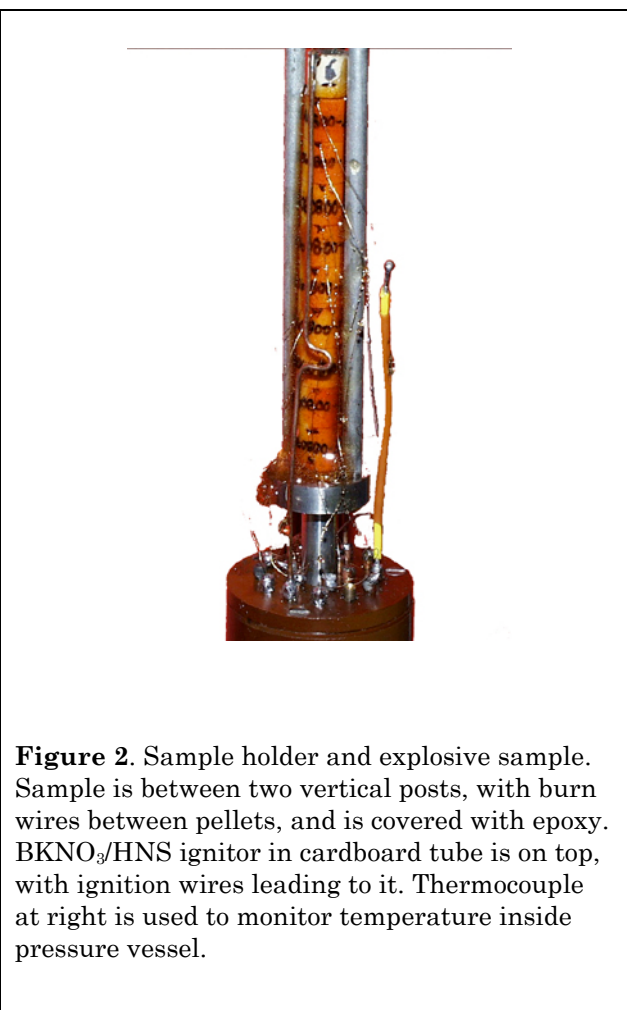
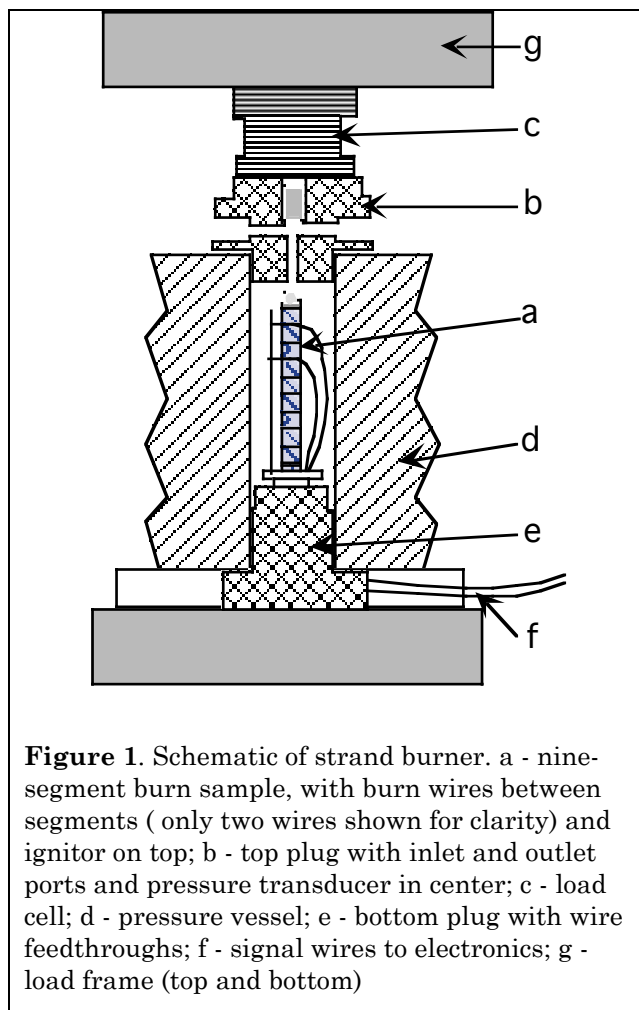


Figure 3. Typical data from strand burner, showing temporal pressure behavior and flame-front time-of-arrival signals.

Inspection of the data in Figure 3 offers a consistency check of the pressure and burn-wire signals. The burn wire data should cover the time span of increasing pressure signal – any significant deviation from this indicates anomalous behavior. For example, sometimes the burn wires all report well before the pressure signal reaches its maximum. This indicates that the burn

front has passed rapidly through the entire sample leaving unburned material that reacts later; this is usually interpreted to be the result of physical deconsolidation or failure of the physical integrity of the sample under pressure. Alternatively, this could represent flame propagation down the side of the sample, although the presence of the epoxy inhibitor should prevent this. To calculate burn rate as a function of pressure, we use the length and time-of-arrival for each pair of pellets (to smooth the results) and calculate the average pressure for this segment of the sample.

MATERIALS

HMX-based explosives tested in this work are listed in Table 1, along with several formulation details. Representative distributions of particle sizes are shown in Figure 4, and the distribution of each formulation is shown in Table 1. Samples were uniaxially pressed in a standard steel die at temperature of 95-105°C and pressures of 200 MPa (30,000 psi), and had densities of typically 98% of the theoretical maximum density for that material.

Table 1. HMX-based explosives for which deflagration measurements are reported

Material	Wt. % HMX	Binder	HMX particle size distribution	Typical density (98% of theoretical maximum)
LX-11	80	Viton A	“LX-04”	1.85
LX-04	85	Viton A	“LX-04”	1.85
RX-04-AN	85	Viton A	“LX-10”	1.85
LX-07	90	Viton A	“LX-04”	1.85
LX-10	95	Viton A	“LX-10”	1.86
PBX-9501	95	50% Estane, 50% BDNPA/F	“PBX-9501”	1.82

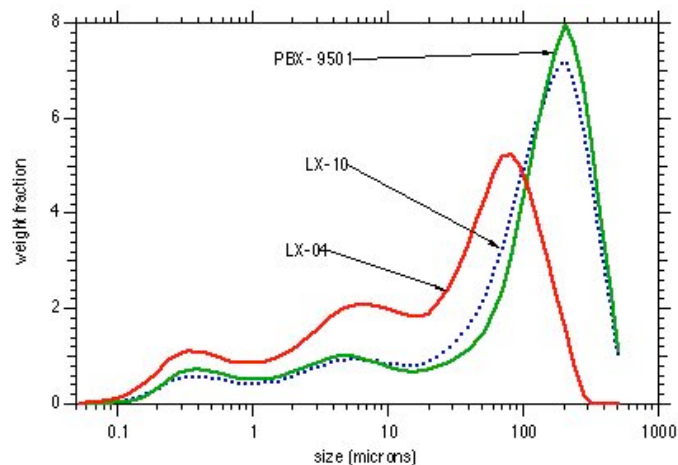


Figure 4. Particle size distribution of different HMX formulations

RESULTS

Deflagration rate data as a function of pressure at ambient temperature are shown below for each material in Table 1. Results for LX-04, LX-11, and RX-04-AN are shown in Figure 5. Also shown in Figure 5 is a dotted line representing a fit to the LX-04 data. Our data are most complete for LX-04 and it exhibits uniform deflagration over the entire pressure range, so this line is included on the other figures as a reference. Figure 6 shows the deflagration rate for LX-07, Figure 7 for LX-10, and Figure 8 for PBX-9501.

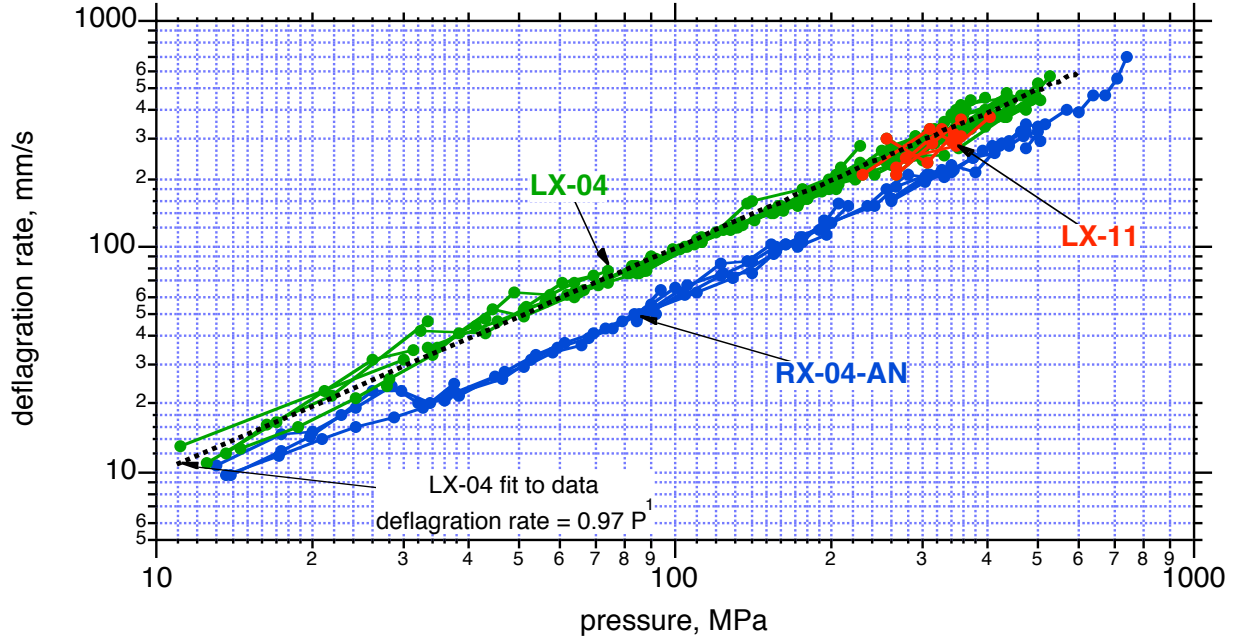


Figure 5. Deflagration rate data for LX-04, LX-11, and RX-04-AN.

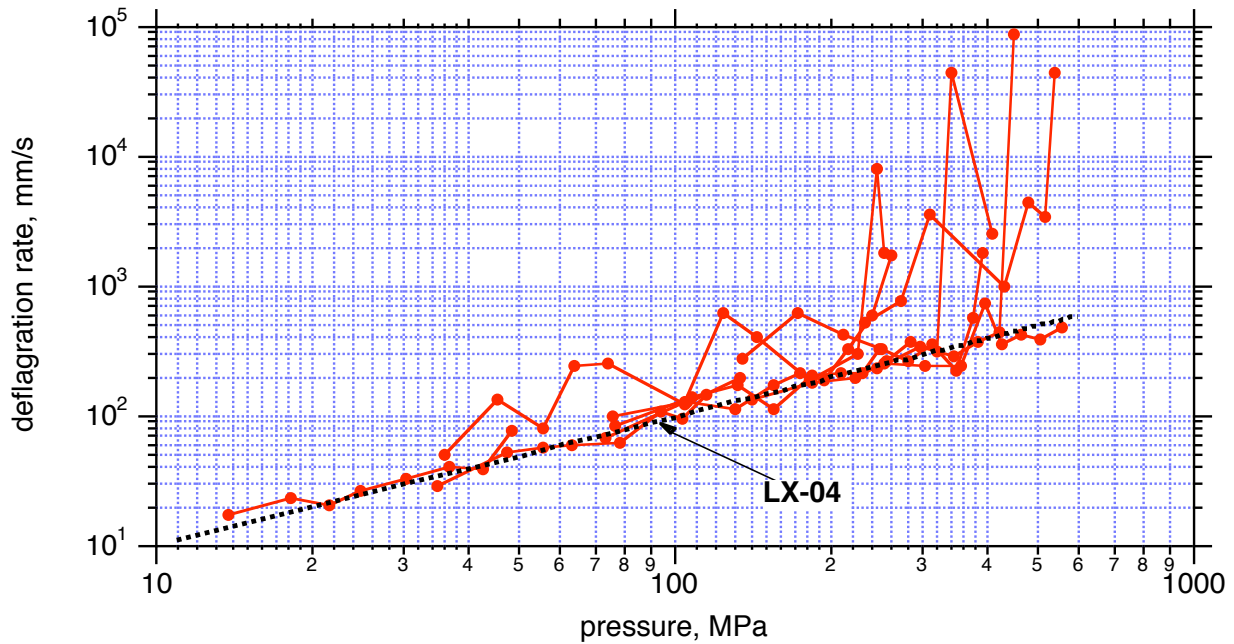


Figure 6. Deflagration rate data for LX-07.

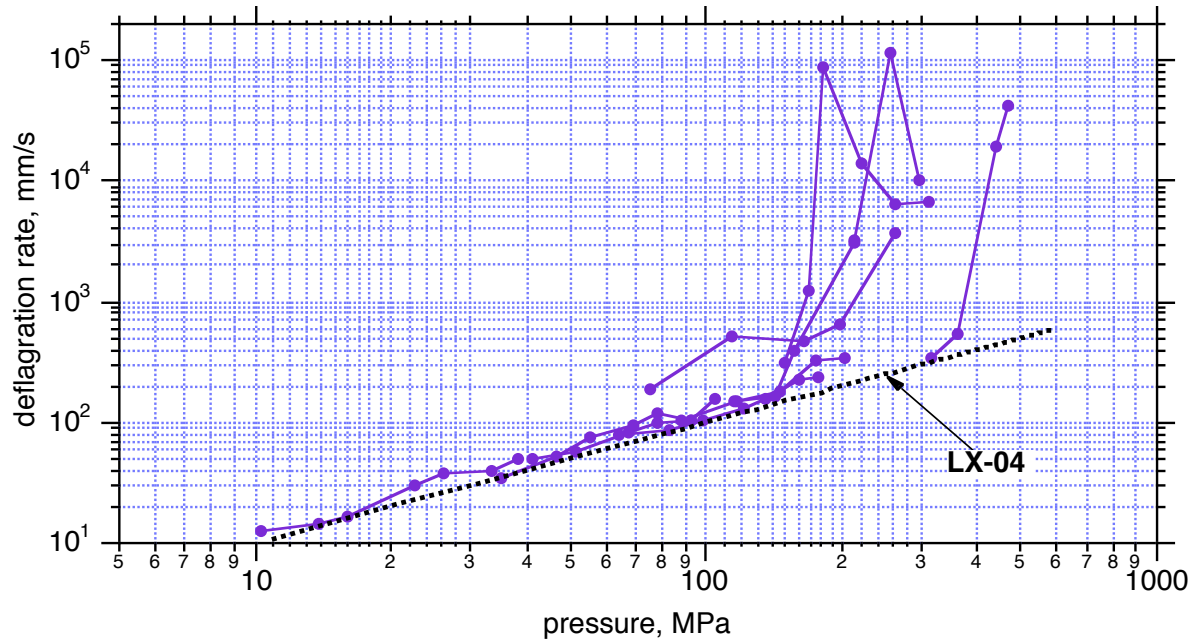


Figure 7. Deflagration rate data for LX-10.

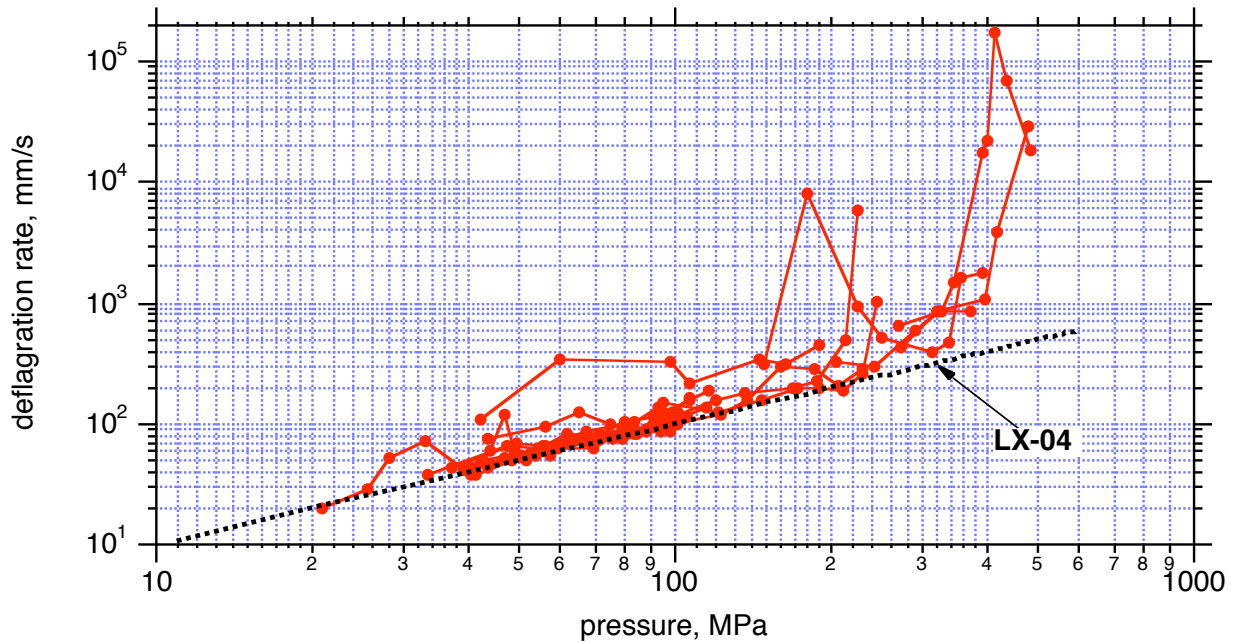


Figure 8. Deflagration rate data for PBX-9501.

Our measurements with heated samples were limited to LX-04, because its uniform behavior at ambient temperature simplifies the identification of temperature effects. The results with samples heated to 150°C and 167°C are shown in Figure 9. Additional samples were heated for 22 hours at temperatures ranging from 155-180°C before measurements were made – the data from these thermally-damaged samples are shown in Figure 10.

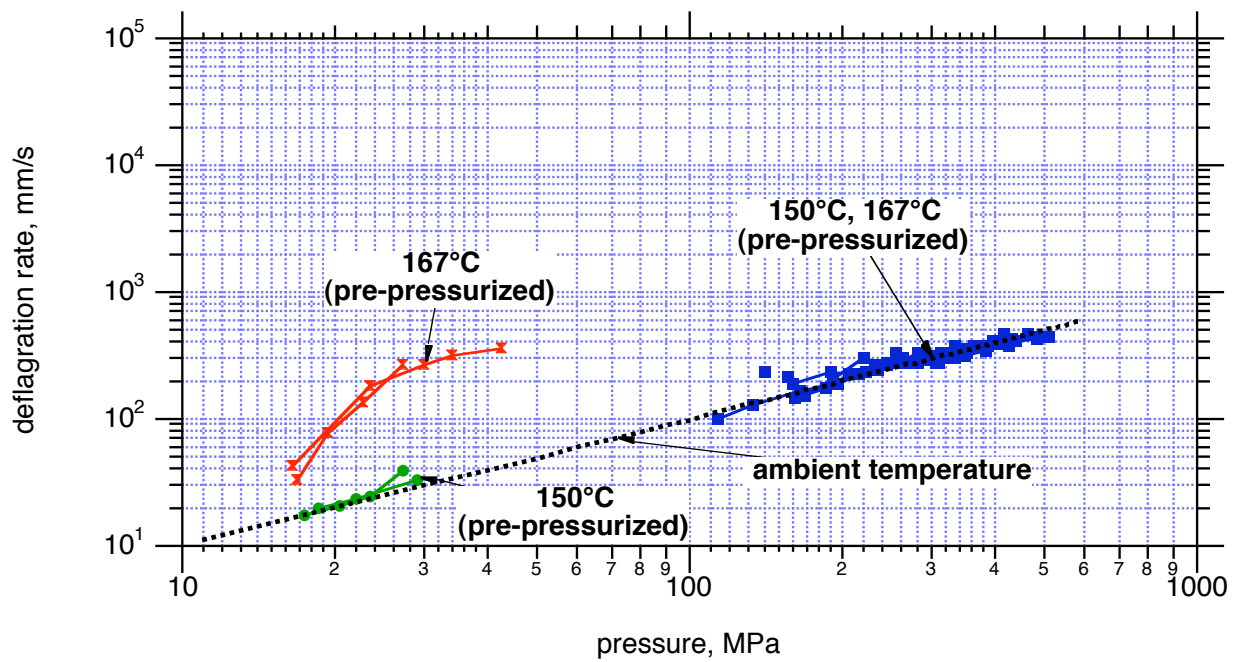


Figure 9. Deflagration rate data for heated LX-04.

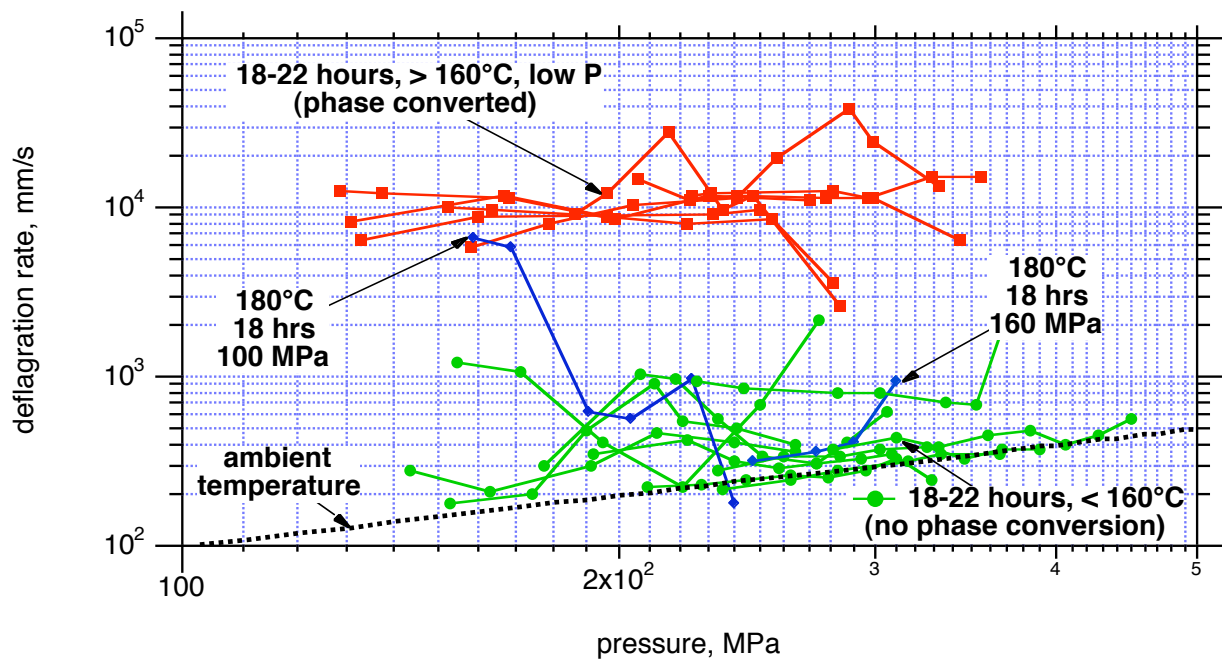


Figure 10. Deflagration rate data for thermally-damaged LX-04.

DISCUSSION

AMBIENT TEMPERATURE RESULTS

The deflagration behavior of LX-04 at ambient temperature is uniform and regular, as seen in Figure 5. The data consistently show a laminar deflagration front progressing through the sample over the entire pressure range. LX-11, which contains more binder (20% vs 15%) but is otherwise identical, exhibits very similar behavior, with perhaps a slightly reduced deflagration rate, although we did not study it over as wide a range of conditions. Measurements with RX-04-AN were designed to determine if the presence of large particles in the HMX leads to rapid deflagration through physical failure of the samples by crystal fracture. As seen in Figure 5, this was not the case – this material showed uniform and regular deflagration over the entire pressure range, albeit with a slower rate than LX-04. This slower rate is expected, and indicates that the large crystals remain intact during deflagration – larger particles have smaller surface-to-volume ratios, and deflagration occurs at the crystal surface as long as the crystal remains intact.

For materials with the same components, but lower in binder (LX-07, Figure 6 and LX-10, Figure 7), the deflagration is very similar to that of LX-04 at lower pressure. However, at pressures above ~ 150 MPa (22,000 psi) the deflagration becomes very rapid and erratic, increasing 10-100-fold in some segments of the sample as measured by burn wire data. In many of these runs the flame front passes through the sample well before the entire sample is consumed. This behavior, called deconsolidative burning, represents the loss of physical integrity of the material at high pressure, with the resultant fracturing, formation of small particles with high surface area, and rapid deflagration through the increased-porosity sample. From these data we conclude that a binder content of > 10% by weight is needed to avoid deconsolidative burning, at least for the Viton A binder used here. We note that the deflagration rate of LX-10 is essentially the same as LX-04 at low pressures, and is significantly higher than that of RX-04-AN, which has the same particle size distribution as LX-10 and the same composition as LX-04. Apparently the slowing of deflagration in LX-10 by the presence of larger particles is coincidentally offset by the effect of the higher HMX content when compared to LX-04.

PBX-9501, which has a high HMX content (95 weight %) and a binder (Estane) heavily plasticized with an energetic plasticizer, shows similar behavior to that of LX-07 and LX-10 (Figure 8). Here the binder composition is quite different, but apparently the low binder content dominates the behavior and the onset of physical deconsolidation. The presence of the energetic binder does not significantly increase the deflagration rate over that of LX-10 or LX-07.

ELEVATED TEMPERATURE RESULTS

The deflagration behavior of heated LX-04 is shown in Figure 9, for samples that were pressurized to the starting pressure while at ambient temperature, then heated to the final temperature and ignited. For initial pressures over 100 MPa (15,000 psi), the deflagration rates are perhaps slightly higher for the hot samples than for the ambient temperature samples, and the same is true for low initial pressures and a temperature of 150°C. However, for samples at low initial pressures and a temperature of 167°C, the deflagration behavior is much faster and erratic, indicative of deconsolidation. This is explained by the beta-to-delta solid-solid phase transition in HMX. The onset temperature for this phase conversion at ambient pressure is ~ 160°C, but because the density decreases about 6% with phase conversion, the transition temperature increases as pressure increases.⁴⁻⁸ From thermodynamic data, Reaugh estimated that a 200 MPa (30,000 psi) pressure would increase the phase transition temperature by several 10's of degrees Celsius.⁹ Therefore, in the experiments in Figure 9 which were pressurized to > 100 MPa before heating, the phase conversion was prevented during the subsequent heating to 167°C; the data represent the deflagration of LX-04 with beta-phase HMX at the reported temperatures. Similarly, for the experiments in Figure 9 with low initial pressures and initial temperature of 150°C, the HMX

remained in beta phase. However, for the experiments with low initial pressure and initial temperature of 167°C, the HMX did apparently convert to delta phase, with a 6% volumetric increase. The volume expansion of the randomly-oriented HMX crystals leads to irregular growth and physical disruption of the sample, with loss of physical integrity and formation of increased surface area. This, in turn, leads to deconsolidative deflagration, similar to that seen in low-binder formulations at high pressures and ambient temperature.

The effect of thermal damage from prolonged heating of LX-04 is shown in Figure 10. Samples heated for 22 hours at temperature < 160°C show somewhat increased deflagration rates (about 3-fold faster), which result from thermal degradation since this temperature is too low to drive the phase conversion. A sample heated for 22 hours at 180°C at 160 MPa (24,000 psi) showed deflagration behavior similar to that of samples heated at < 160°C, indicating that the effect of thermal damage was only slightly increased by the 20°C higher temperature. A sample heated for 22 hours at 180°C at 100 MPa (15,000 psi) showed rapid deflagration at the beginning of the run and a rapidly decreasing deflagration rate as the reaction proceeded (despite an increase in pressure). This may indicate that the sample was just beginning to phase convert, and that the increase in pressure during deflagration was sufficient to reverse the phase conversion during the experiment. The latter part of that interpretation is speculative, however; another explanation is a temperature gradient along the sample with highest temperature (and phase conversion) at the top (where it is ignited). We do not have sufficient data to distinguish between these explanations. Finally, many runs were made with samples heated for 18-22 hours at temperature above 160°C at ambient pressure. These all showed greatly-increased deflagration rates (about 40-fold faster), resulting from the phase transition and loss of physical integrity of the samples.

Our complete results (including some not in Figure 10) are summarized in Table 2, below. The deflagration rate of LX-04 at temperatures up to 180°C with no prolonged exposure to high temperature and no phase conversion is little-changed from that at ambient temperature; in the runs at 180°C with no soak there was insufficient time for the phase conversion to take place, so the samples were tested in the initial beta phase. With prolonged heating in the absence of phase conversion, thermal damage leads to increased deflagration rates, about 3 times faster after 22 hours at 150-155°C and about 10 times faster at 180°C. The beta-to-delta phase transition has the biggest effect on deflagration behavior, with an approximately 40-fold increase following phase conversion.

Table 2. Summary of the effect of heating on deflagration behavior of LX-04.

Initial deflagration pressure, MPa	Temp., °C	Soak time, hours	Soak P, MPa	Phase change?	Replicates	Normalized rate
10-250	150-160	0	-	No	14	1
100-250	150-155	18-22	0.1-150	No	7	3
100-265	180	0	-	No	8	1
130-160	180	18-22	130-160	No	2	10
130	180	18-22	0.1	Yes	6	40

EXAMINATION OF TEMPORAL PRESSURE DATA

The pressure-time data collected for each experiment provides additional information on the deflagration process. For example, erratic or very rapid pressure increases indicate deconsolidative deflagration. Inasmuch as the increased reaction rate during deconsolidative deflagration represents an increase in burning surface area from physical fracture, comparison of the rates of pressure

increase for deconsolidative and uniform deflagration allows a quantification of the increase in surface area resulting from deconsolidation (following the well-known vivacity concept in combustion^{10, 11}). These analyses are underway for the experiments reported here, and will be the subject of a future paper.

CONCLUSIONS

The deflagration rate data reported here, taken with several different HMX formulations over a wide range of pressures and temperatures, allow identification of key factors controlling deflagration behavior. LX-04 provides an excellent baseline behavior – its small particle size distribution and high binder content result in uniform and regular deflagration. Formulation variations from this material provide insight into the importance of different factors. The key formulation variable is the quantity of binder present – formulations with less than 15% binder by weight exhibit very rapid deconsolidative deflagration at pressures above 100-150- MPa. The HMX particle size and the HMX content also play a role, with larger particles and lower HMX content giving slower deflagration rates. We could not distinguish a difference between an inert and reactive binder at ambient temperature.

Temperature effects are also important in deflagration behavior. Deflagration at elevated temperatures does not show a significant increase in rate, but thermal damage by prolonged heating increases deflagration rates several-fold. If the beta-to-delta phase transition takes place, the effect is even more severe.

In a thermal explosion, in which an explosive is heated sufficiently to cause a rapid and violent reaction, the predominant reaction mechanism is deflagration at high pressures. In cases with slow heating rates, the reaction is also occurring at heated explosive, while in cases with fast heating rates much of the reaction will propagate in unheated explosive. Therefore, characterization of the high-pressure deflagration behavior of explosives at ambient and elevated temperatures provides insight into the propagation of thermal explosions in those same materials.

ACKNOWLEDGEMENTS

We gratefully acknowledge financial support for this work by the LLNL High Explosives Surety Project and the Office of Munitions Program. Key contributors to this experimental effort include Kevin Black, Les Calloway, Martin DeHaven, Greg Sykora, and Kou Moa. We also thank Al Nichols and Jack Reaugh for fruitful discussions of the work as it progressed.

REFERENCES

1. J.L. Maienschein and J.B. Chandler, "High Pressure Laminar Burn Rates of AP/Al/HTPB Propellants," in *Proceedings of JANNAF 34th Combustion and 16th Propulsion Systems Hazards Subcommittee Meetings*, West Palm Beach, FL, CPIA, Publication 657, Vol. II, p. 95 (1997).
2. J.L. Maienschein and J.B. Chandler, "Burn Rates of Pristine and Degraded Explosives at Elevated Pressures and Temperatures," in *Proceedings of 11th International Detonation Symposium*, Snowmass, CO, Office of Naval Research, p. 872 (1998).
3. J.L. Maienschein and J.F. Wardell, "Deflagration Behavior of PBXN-109 and Composition B at High Pressures and Temperatures," in *Proceedings of JANNAF 38th Combustion and 20th Propulsion Systems Hazards Subcommittee Meetings*, Sandestin, FL, CPIA, Publication ##, p. (2002).

4. H.H. Cady, A.C. Larson and D.T. Cromer, "The crystal structure of alpha-HMX and a refinement of the structure of beta-HMX," *Acta Cryst.*, 16, 617 (1963).
5. T.B. Brill and R.J. Karpowicz, "Solid phase transition kinetics: the role of intermolecular forces in the condensed phase decomposition of octahydro-1,3,5,7-tetranitro-1,3,5,7-tetrazocine," *J. Phys. Chem.*, 86, 4260 (1982).
6. T.B. Brill and C.O. Reese, "Analysis of intermolecular interactions relating in the thermophysical behavior of alpha, beta, and delta octahydro-1,3,5,7-tetranitro-1,3,5,7-tetrazocine," *J. Phys. Chem.*, 84, (1980).
7. W.C. McCrone, "Crystallographic Data: Cyclotetramethylene Tetranitramine (HMX)," *Analytical Chem.*, 22, 1225 (1950).
8. A.S. Teetsov and W.C. McCrone, "The Microscopical Study of Polymorph Stability Diagrams," *Microscop. Cryst. Front.*, 15, 13 (1965).
9. J.E. Reaugh, Lawrence Livermore National Laboratory, personal communication, July 1, 1999.
10. A. Birk, D.E. Kooker and P. Baker, "Model of Cavity Combustion Within an Energetic Solid: Application to Composition-B," in *Proceedings of JANNAF 37th Combustion and 19th Propulsion Systems Hazards Subcommittee Meetings*, Monterey, CA, CPIA, Publication 704, Vol. II, p. 95 (2000).
11. R. Lieb and P. Baker, "Combustion Morphology of TNT and Composition B," in *Proceedings of JANNAF 37th Combustion and 19th Propulsion Systems Hazards Subcommittee Meetings*, Monterey, Ca, CPIA, Publication 704, Vol. II, p. 81 (2000).